International Journal of Thermophysics, Vol. 19, No. 1, 1998

Conventional Simultaneous Measurement of Specific Heat Capacity and Thermal Conductivity by Thermal Radiation Calorimetry

K. Hisano,[1,2] S. Sawai,[1] and K. Morimoto[1]

Received October 23, 1997

Thermal radiation calorimetry has been applied to measure the thermal conductivity and the specific heat capacity of an isolated solid specimen simultaneously. The system, in which a disk-shaped specimen and a flat heater are mounted in a vacuum chamber with the specimen heated on one face by irradiation, is presented. A theoretical formulation of the simultaneous measurement at quasi-steady state is described in detail. Noncontact temperature measurement of both specimen surfaces has been performed using pyrometers and a thermocouple set in the gap between the heater and the specimen. Pyroceram 9609 specimens, whose surfaces were blackened with colloidal graphite, were used in the measurement. The largest error involved in the noncontact temperature measurement is ± 2°C in the range from 450 to 650°C. The resultant values of the specific heat capacity and the thermal conductivity deviate by about 10% from the recommended values for the Pyroceram specimen.

KEY WORDS: calorimetry; emissivity; high temperature; specific heat capacity; thermal conductivity.

1. INTRODUCTION

Thermal radiation power emitted from a material depends on its surface emissivity. If the specimen is heated only by thermal radiation and the input power is evaluated properly, the thermophysical properties of materials can be determined. Heat capacity measurements have been performed in a transient state for a disk-shaped isolated specimen using a calorimeter based on thermal radiation heating [1, 2]. This calorimeter has also been applied to thermal conductivity measurements in the quasi-steady

[1] Department of Mathematics and Physics, National Defense Academy, Hashirimizu 1-10-20, Yokosuka 239, Japan.

[2] To whom correspondence should be addressed.

0195-928X/00/0700-0291$18.00/0

state [3, 4] as well as the steady state [5]. The system, in which a disk-shaped specimen and a heater are mounted in a vacuum chamber and the specimen is heated at one face by irradiation, is considered in this calorimeter. As is usual in the case of heat capacity measurements, the specimen temperature is changed slowly at a constant time rate during measurement of thermal conductivity in the quasi-steady state. It may, therefore, be possible to develop a conventional method of simultaneous measurement of the specific heat capacity and the thermal conductivity. Because of the one-face irradiation, a temperature difference between both surfaces of an isolated specimen at high temperature is always observed. Therefore, the measured specific heat capacity will be a value averaged in this temperature range. In this paper, a theory to perform simultaneous measurement at quasi-steady state is described. Results of the measurement by means of a noncontact technique are shown for Pyroceram 9606 specimens.

2. THEORETICAL FORMULATION

Two basic equations are required to discuss the heat diffusion in a specimen. The first is the energy conservation equation, given as

$$\frac{\partial q}{\partial t} + \operatorname{div} j_q = 0 \tag{1}$$

where q and j_q are the heat energy per unit volume and the heat current, respectively. The second is a phenomenological relation. That is,

$$j_q = -\lambda \operatorname{grad} T \tag{2}$$

where λ and T are the thermal conductivity and the temperature, respectively. Consider a one-dimensional system in which a specimen of thickness L is heated on one face by irradiation at a low temperature change rate (see Fig. 1); then the above two equations combine to give

$$C_p \rho \frac{\partial T}{\partial t} = \frac{\partial}{\partial x}\left(\lambda \frac{\partial T}{\partial x}\right) \tag{3}$$

where C_p and ρ are the specific heat capacity and the density, respectively. The thermal conduction in the direction parallel to the faces is neglected in the above equation. The energy exchange at the back specimen surface ($x = 0$), facing the chamber wall maintained at room temperature, is written as

$$\lambda \left(\frac{\partial T}{\partial x}\right)_0 A = \varepsilon I_0 A \tag{4}$$

where ε and A are the surface emissivity and the specimen surface area, respectively. The radiant power emitted by the specimen to the chamber wall at room temperature for a perfect absorber I is

$$I = \sigma(T^4 - T_r^4) \tag{5}$$

where σ and T_r are the Stefan–Boltzmann constant and room temperature, respectively. Similarly, the energy exchange at the front surface ($x = L$), facing the heater, is given as

$$\lambda \left(\frac{\partial T}{\partial x}\right)_L A = E_h(I_h - I_L)\, A - E_s I_L A - \frac{dQ_L}{dt} \tag{6}$$

where E_h and E_s are the "effective" emissivities defined in the present paper and dQ_L/dt is the heat loss through the specimen support. E_h and E_s depend on the configuration between the heater and the specimen and the surface emissivities. Equation (6) is the result obtained from the calculation based on the net-radiation method [6, 7], assuming that the reciprocal relation is held among the configuration factors because of the high emissivity of the blackened specimen surfaces [8]. Therefore, the effective emissivities are constant as long as the configuration and the surface emissivities are the same. In the quasi-steady state when the specimen temperature is changed slowly at a constant change rate, the differences in the time and the spatial change rates between both surfaces are much smaller than those rates averaged with position x. These are expressed as

$$\left|\left(\frac{dT}{dt}\right)_L - \left(\frac{\partial T}{\partial t}\right)_0\right| \ll \left|\left(\frac{\partial T}{\partial t}\right)_{av}\right| \quad \text{and} \quad \left(\frac{\partial T}{\partial x}\right)_L - \left(\frac{\partial T}{\partial x}\right)_0 \ll \left(\frac{\partial T}{\partial x}\right)_{av} \tag{7}$$

where the subscript "av" indicates the averaged value. Therefore, Eq. (3) gives the following relation for the quasi-steady state approximation:

$$C_p \rho L \left(\frac{\partial T}{\partial t}\right)_{av} = \lambda \left\{\left(\frac{\partial T}{\partial x}\right)_L - \left(\frac{\partial T}{\partial x}\right)_0\right\} \tag{8}$$

Similarly, the temperature difference between the surfaces is given as

$$T_L - T_0 = L \left(\frac{\partial T}{\partial x}\right)_{av} \tag{9}$$

Consider both heating and cooling modes of the specimen temperature change; Eqs. (3), (4), and (6) derive the following relation for the specific

heat capacity at the same front surface temperature, ($T_L = T'_L$) because of small changes in C_p and ρ with temperature for a regular material:

$$C_p = \frac{E_h(I_h - I'_h) - \varepsilon(I_0 - I'_0)}{\rho L\{(\partial T/\partial t)_{av} - (\partial T'/\partial t)_{av}\}} \tag{10}$$

where the superscript $'$ refers to the cooling mode. The heat loss through the specimen support is largely canceled in the above equation because of the same temperature. Because the time and the spatial rates of temperature change are monotonically increasing or decreasing functions of position x, we may assume that the averaged rates are given as

$$\left(\frac{\partial T}{\partial t}\right)_{av} = \frac{1}{2}\left\{\left(\frac{\partial T}{\partial t}\right)_L + \left(\frac{\partial T}{\partial t}\right)_0\right\} \quad \text{and} \quad \left(\frac{\partial T}{\partial x}\right)_{av} = \frac{1}{2}\left\{\left(\frac{\partial T}{\partial x}\right)_L + \left(\frac{\partial T}{\partial x}\right)_0\right\} \tag{11}$$

Therefore, Eqs. (4), (8), and (9) give

$$\lambda \frac{T_L - T_0}{L} = \varepsilon I_0 + \frac{1}{2} C_p \rho L \left(\frac{\partial T}{\partial t}\right)_{av} \tag{12}$$

The above equation is valid only for the case where the first term on the right-hand side is much larger than the second term. In other words, the quasi-steady state approximation requires that the incoming or outgoing radiant power must be much larger than that absorbed or emitted in the specimen. Similar to the heat capacity measurement, considering both heating and cooling modes of the temperature change, the above equation derives the following relation at the same back surface temperature ($T_0 = T'_0$) if the temperature change rate is the same for both modes:

$$\lambda = \frac{2L}{T_L + T'_L - 2T_0} \varepsilon I_0 \tag{13}$$

Equations (10) and (13) imply that it is possible to measure the specific heat capacity and the thermal conductivity simultaneously because all quantities on the right-hand sides of the equations are measurable at the same time.

3. NONCONTACT MEASUREMENT

A value of E_h for the blackened surface at various temperatures is required and a heat capacity measurement of a high conductivity substance

whose specific heat capacity is well known is used to obtain the values. Because of the high thermal conductivity, no significant temperature gradient in the specimen is expected even though the irradiation is on one face. Therefore, E_h is derived from Eq. (10) setting $T_0 = T'_0$. It is also necessary to measure both surface temperatures of the insulating specimen. The back surface temperature T_0 is measured using a pyrometer, while the front surface temperature T_L is obtained from the heater temperature T_h and the temperature of the thermocouple T_t placed in the gap between the heater and the specimen. The radiant power exchange among the thermocouple junction, the heater, the specimen, and the chamber wall is expressed as

$$e_1(I_h - I_t) = e_2(I_t - I_L) + \frac{dQ_t}{dt} + e_3 I_t \tag{14}$$

where e_1, e_2, and e_3 are coefficients of the emissive (or absorption) power. dQ_t/dt is the heat loss through the thermocouple leads. The heat capacity of the thermocouple junction is ignored in the above equation. The analytical form of the above equation is also derived from the calculation based on the net-radiation method as Eq. (6) is derived. Assuming the heat loss through the leads to be much smaller than the radiant powers, Eq. (14) can be rewritten as

$$I_L = \alpha(T_t)\, I_t - \beta I_h \tag{15}$$

where $\alpha(T_t) = \{e_1 + e_2 + e_3 + (dQ_t/dt)/I_t\}/e_2$ and $\beta = e_1/e_2$. Therefore, a noncontact measurement of the front surface temperature is performed with the values of $\alpha(T_t)$ and β at various temperatures. If the heater radiation power W_h is measured instead of the heater temperature T_h, I_h in Eq. (15) is replaced by W_h/G_h, where G_h $(= W_h/I_h)$ is the gain factor of the electrical circuit for the pyrometer.

4. EXPERIMENTAL

The apparatus used in the present experiment has been described in detail in a previous paper [5]. The specimen, supported by alumina tubes (1 mm in diameter), is placed 6 mm above the heater made from a graphite sheet (5 cm square and 0.5 mm in thickness). The heater part is shown schematically in Fig. 1. A Pt–13% Rh thermocouple (0.1 mm in diameter) is set about 1 mm below the front specimen surface. A radiation shield made from a copper sheet is used in the present experiment to achieve a

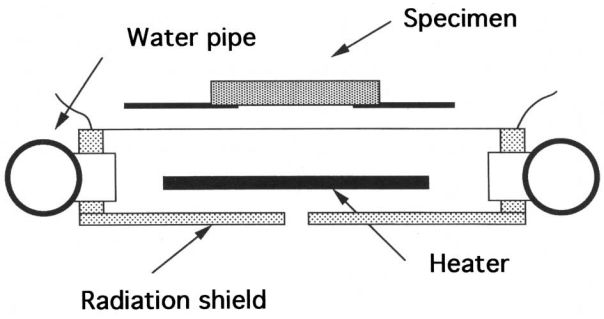

Fig. 1. Heater part of the apparatus.

high heater efficiency. Surfaces of all specimens are blackened with colloidal graphite (Electrodag 188; Acheson) at a density of $2\ \text{mg} \cdot \text{cm}^{-1}$, yielding a velvet-like surface after evaporation of the acrylic binder above 400°C. The calibration of the surface emissivity ε is performed by measuring the infrared spectral reflectivity at room temperature. The estimated emissivity shows a small temperature change between 92 and 96% in the range from 300 to 800°C [8]. The heater current is controlled so that the change rate becomes about $5°\text{C} \cdot \text{min}^{-1}$ for both heating and cooling modes. The data are collected every 15 s so that a temperature interval between the datum points becomes approximately 1.2°C.

5. RESULTS AND DISCUSSION

A copper specimen (3 mm thick and 25 mm in diameter) on which the thermocouple was attached was prepared to obtain the value of E_h/G_h from the heat capacity measurement. The data set for T_s, T_t, and W_h was collected at various temperatures for both modes, where T_s is the specimen temperature. Differences in W_h between the modes and the temperature change rates for heating and cooling at the same specimen temperature are shown in Fig. 2. Figure 3 shows the value of E_h/G_h estimated from the results shown in Fig. 2. The values of the specific heat capacity of copper metal were taken from the literature [9]. It is clearly shown that E_h/G_h is almost constant, with a value of 7.5.

Two sets of data for I_s and W_h (or I_h) at a certain thermocouple temperature T_t are required to obtain the values of $\alpha(T_t)$ and β. Therefore, two copper specimens (1.5 mm thick and 25 mm in diameter), on which the

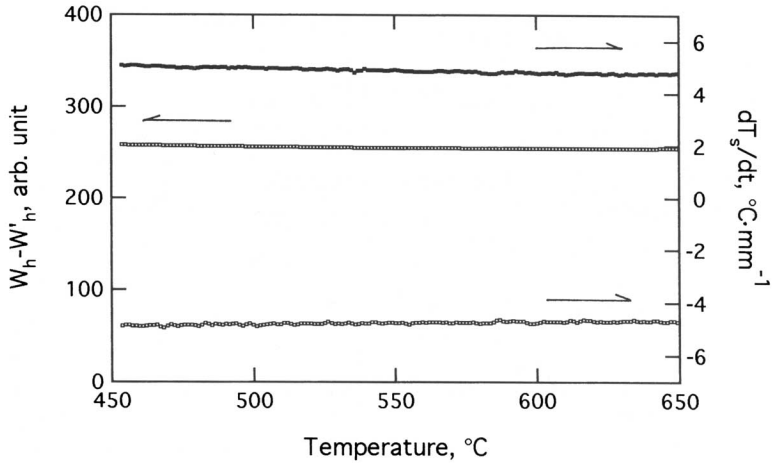

Fig. 2. Temperature dependences of $W_h - W'_h$ and dT_s/dt: (■) heating mode; (□) cooling mode.

thermocouple was attached, were prepared. Both surfaces of one specimen (Cu 1) were blackened, while the front surface of another specimen (Cu 2) was blackened in the same way as Cu 1 but a polka dot print was made on the back surface [4, 5]. The data set for T_s, T_t, W_h, and W_s of both specimens was collected for heating and cooling. Figure 4 shows $G_s(=W_s/I_s)$ at various specimen temperatures for the Cu 1 specimen. Only

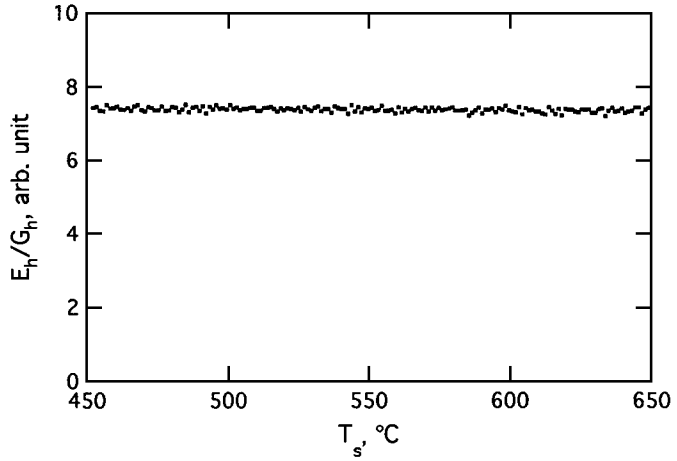

Fig. 3. Temperature dependence of E_h/G_h.

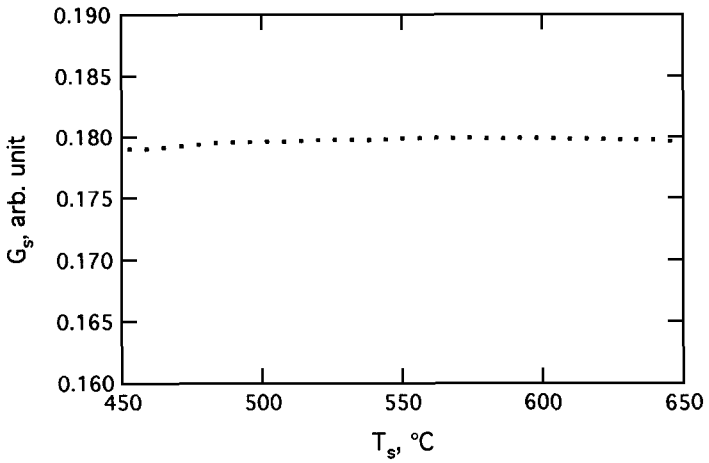

Fig. 4. Temperature dependence of G_s. Only some of the data are plotted.

some of the data are plotted in Fig. 4. The result shown was used to make the noncontact measurement of the back surface temperature. No hysteresis was observed for either mode within the experimental errors. The accuracy of the temperature measurement of the back surface is $+0.5$°C as long as the surface emissivity is the same. Figure 5 shows the temperature

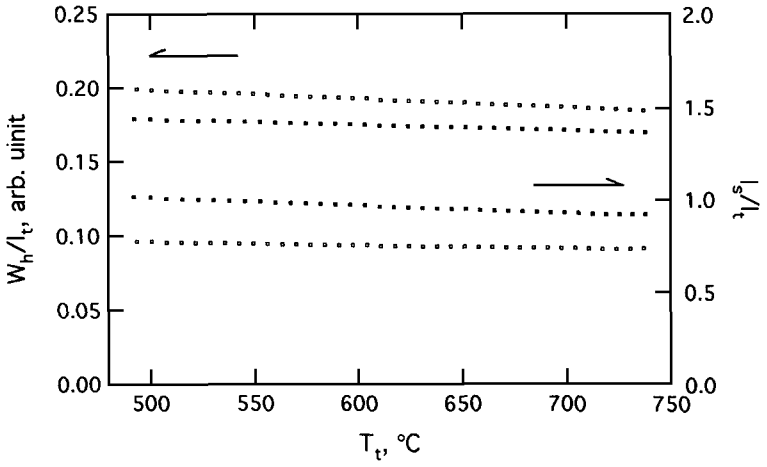

Fig. 5. Temperature dependences of W_h/I_t and I_s/I_t for the heating mode: (■) Cu 1; (□) Cu 2. Only some of the data are plotted.

dependences of W_h/I_t and I_s/I_t at various thermocouple temperatures T_t for the heating mode. Equation (15) derives the following relation at the same thermocouple temperature T_t:

$$\frac{\beta}{G_h} = -\frac{I_h - I'_h}{W_h - W'_h} \tag{16}$$

The heat loss term is largely canceled because of the same temperature. Figure 6 shows the temperature dependences of β/G_h estimated from the results shown in Fig. 5 and $\alpha(T_L)$ estimated from Eq. (15) using the value of β/G_h. As shown in Fig. 6, although β/G_h is more or less constant with temperature, $\alpha(T_t)$ decreases slightly with temperature. This is caused by the heat loss through the thermocouple leads. Hysteresis is observed in these quantities for heating and cooling, unlike the case for the steady state [5]. This is caused mainly by the heat capacity of the thermocouple junction, which was ignored in the derivation of Eq. (14). To evaluate the accuracy of this noncontact measurement, the deviation of the calculated value from the experimental value for the 3-mm-thick copper specimen described above was estimated considering the hysteresis. Results, indicating a largest deviation of ± 1.5°C, are shown in Fig. 7.

Two Pyroceram 9606 specimens (3 and 4.7 mm in diameter and 25 mm thick) were used to confirm the validity of the simultaneous measurement of the specific heat capacity and the thermal conductivity based on Eqs. (10) and (13). The entire surfaces of the specimens were

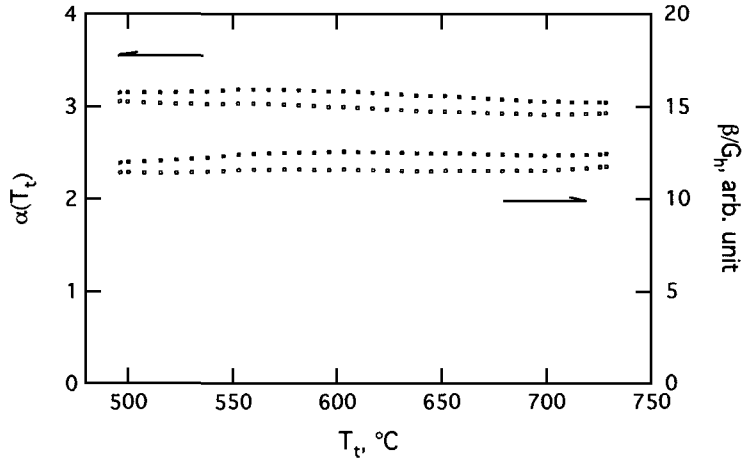

Fig. 6. Temperature dependence of $\alpha(T_t)$ and β/G_h. (■) Heating mode; (□) cooling mode. Only some of the data are plotted.

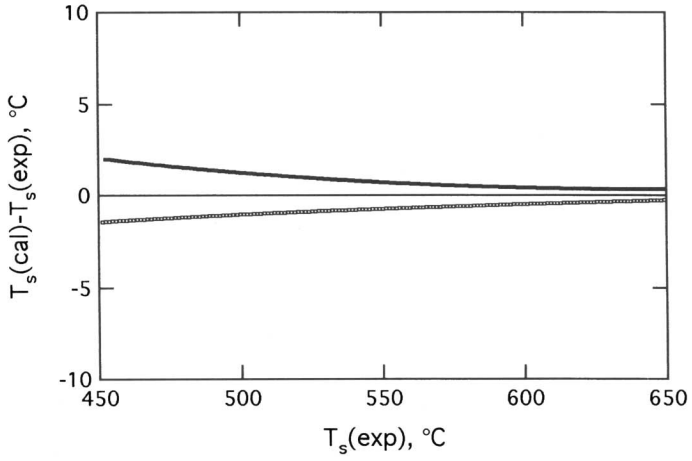

Fig. 7. Temperature deviations obtained by the noncontact measurement from the temperature measured with the thermocouple for the 3-mm-thick copper specimen: (■) heating mode; (□) cooling mode.

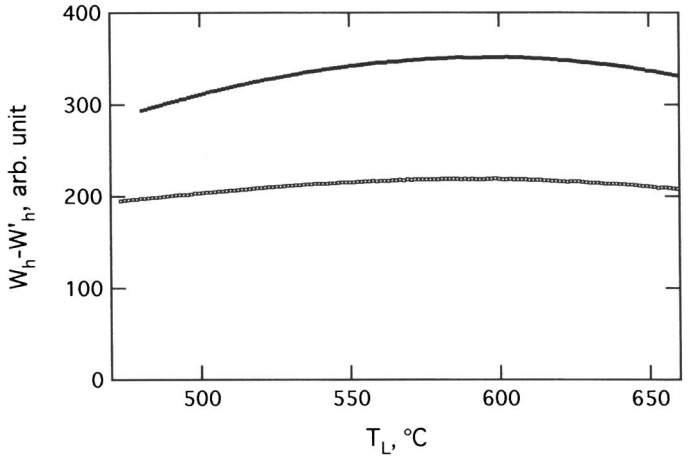

Fig. 8. $W_h - W'_h$ at the same specimen surface temperatures for the Pyroceram specimens: (■) 4.7-mm-thick specimen; (□) 3.0-mm-thick specimen.

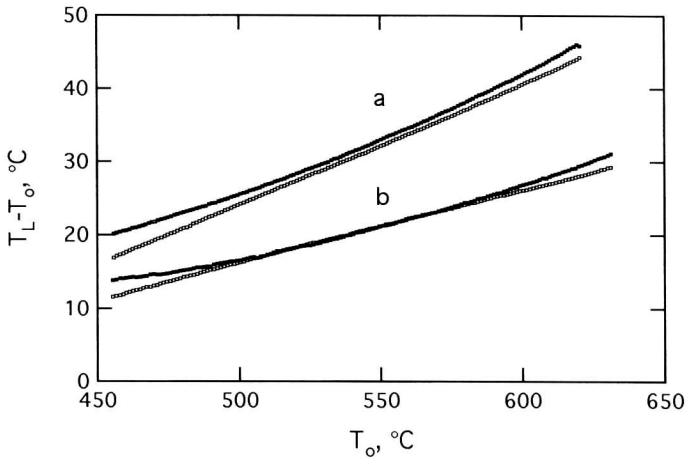

Fig. 9. $T_L - T'_L$ at the same back surface temperatures: (a) the 4.7-mm-thick specimen; (b) the 3.0-mm-thick specimen. (■) Heating mode; (□) cooling mode.

coated with copper metal by vacuum evaporation before blackening to achieve good temperature homogeneity in the surfaces and to reduce the radiation loss from the side surface as much as possible. The data set for T_t, W_h, and W_s was collected for cooling and heating. Figures 8, 9, and 10 show for both specimens the difference in the radiant power from the

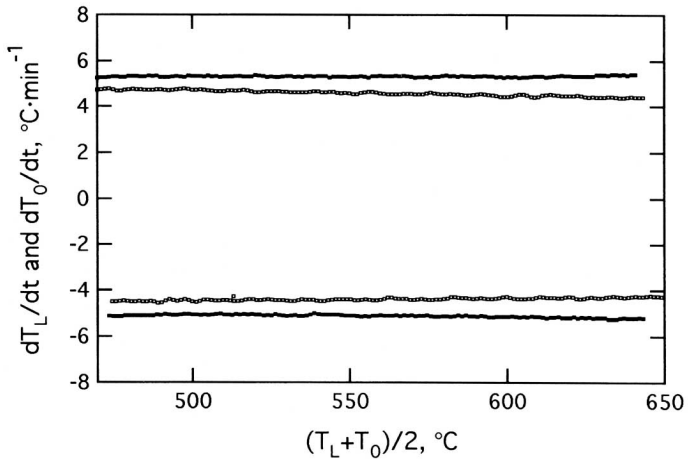

Fig. 10. Temperature change rates at both specimen surfaces: (■) dT_L/dt; (□) dT_0/dt.

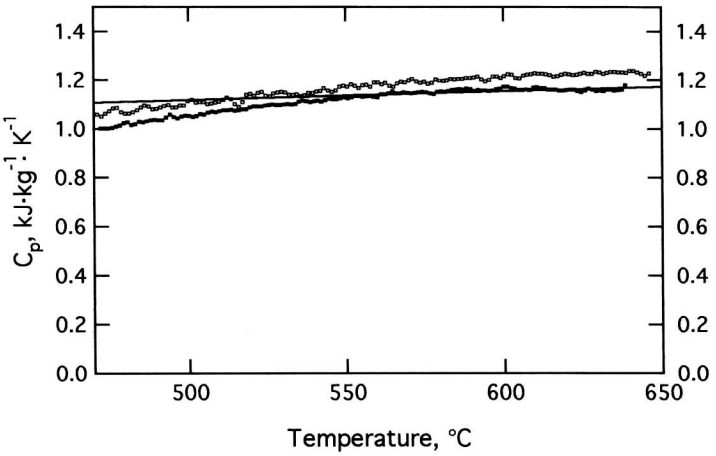

Fig. 11. Temperature dependence of the specific heat capacity of the Pyroceram specimens: (■) 4.7-mm-thick specimen; (□) 3.0-mm-thick specimen. The solid line shows the recommended values.

heater at the same front surface temperature, the temperature differences between the surfaces at the same back surface temperature, and the temperature change rates at both surfaces. Figures 11 and 12 show the temperature dependences of the specific heat capacity and the thermal conductivity obtained simultaneously. The specimen temperature was attributed

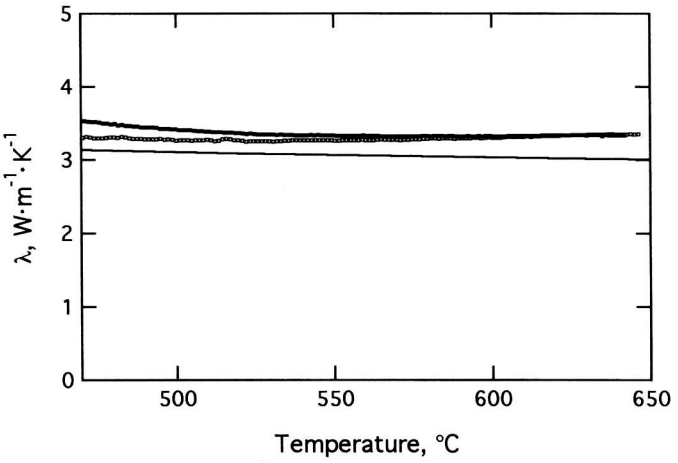

Fig. 12. Temperature dependence of the thermal conductivity of the Pyroceram specimens: (■) 4.7-mm-thick specimen; (□) 3.0-mm-thick specimen. The solid line shows the recommended values.

to the value of $(T_L + T_0)/2$ averaged between the modes. The surface emissivity ε was assumed to be constant, with a value of 94% in the analysis. The solid lines indicate the recommended values taken from the literature [10, 11]. Since the largest error involved in noncontact temperature measurements is about $\pm 2°C$, the results shown in Fig. 9 derive a deviation of ± 10 to $\pm 20\%$ for the thermal conductivity in the present temperature range. As shown in Figs. 11 and 12, the results indicate a maximum deviation of about 10% from the recommended value for both physical quantities.

Once again, the quasi-steady state approximation requires the conditions shown in Eqs. (7) and (11). The largest difference in the time rate of temperature change between the surfaces is about 20% of the averaged rate for the 4.7-mm-thick specimen as shown in Fig. 10, while 10% is estimated for the spatial change rate from Eqs. (4) and (8). To confirm the validity of Eq. (8) particularly, a computer simulation based on the finite difference method [12] has been performed in the present temperature range using the recommended values and ignoring the heat loss term in Eq. (6). The results imply an almost-linear change in both time and spatial temperature change rates.

6. CONCLUSION

A new conventional method based on thermal radiation calorimetry (TRAC) was proposed for the simultaneous measurement of specific heat capacity and thermal conductivity. A theoretical formulation of the measurement at quasi-steady state was described in detail. Noncontact temperature measurements of both specimen surfaces were performed with pyrometers and the thermocouple set in the gap between a flat heater and a specimen. The largest error involved in the noncontact measurement is $\pm 2°C$ in the temperature range between 450 and 650°C. The resultant values of both specific heat capacity and thermal conductivity deviate by about 10% from the recommended values for Pyroceram 9606.

ACKNOWLEDGMENT

The authors are grateful to R. P. Tye for his continuous encouragement on the present subject.

REFERENCES

1. K. Hisano and T. Yamamoto, in *Proc. 12th Japan Symp. Thermophys. Prop., Vol. 12* (Japan Society of Thermophysical Properties, Kyoto, 1991), p. 287.
2. K. Hisano and T. Yamamoto, *High Temp. High Press.* **25**:337 (1993).

3. K. Hisano and F. Placido, *High Temp. High Press.* **30** (1998).
4. K. Hisano, in *Proc. 6th Int. Symp. Temp. Therm. Measurem. Industry Sci.* (Torino, Sept. 10–20, 1996), p. 519.
5. K. Hisano, *Int. J. Thermophys.* **18**:535 (1997).
6. H. C. Hottel and A. F. Sarofim, *Radiative Transfer* (McGraw–Hill, New York, 1967).
7. R. Siegel and J. R. Howell, *Thermal Radiation Heat Transfer* (McGraw–Hill, New York, 1972).
8. K. Hisano, S. Sawai, and K. Morimoto, *Int. J. Thermophys.* **19**:305 (1998).
9. D. E. Gray (ed.), *American Institute of Physics Handbook* (McGraw–Hill, New York, 1972).
10. Y. S. Touloukian and E. H. Buyco, *Thermophysical Properties of Matter, 5, Nonmetallic Solids, Specific Heat* (Plenum, New York, 1972).
11. Y. S. Touloukian, *Thermophysical Properties of Matter, 2, Nonmetallic Solids, Thermal Conductivity* (Plenum, New York, 1972).
12. P. J. Roache, *Computational Fluid Dynamics* (Hermosa, Albuquerque, 1976).